

# A functional hybrid polyoxometalate framework based on a 'trilacunary' heteropolyanion $[(P_4W_6O_{34})_2Co_2Na_2(H_2O)_2]^{18-}$ †

Chris Ritchie,<sup>‡a</sup> Fengyan Li,<sup>‡a,b</sup> Chullikkattil P. Pradeep,<sup>a</sup> De-Liang Long,<sup>a</sup> Lin Xu<sup>\*b</sup> and Leroy Cronin<sup>\*a</sup>

Received 15th April 2009, Accepted 10th June 2009

First published as an Advance Article on the web 9th July 2009

DOI: 10.1039/b907410d

Using multifunctional organocations a novel heteropolyanion,  $[(P_4W_6O_{34})_2Co_2Na_2(H_2O)_2]^{18-}$ , with unprecedented structural features, has been observed, and extension of these clusters from molecules into 1D chains occurs through a dimeric cobalt species, with this material exhibiting reversible colour/magnetic susceptibility changes upon dehydration.

Polyoxometalates (POMs), anionic transition-metal oxide clusters, have received much attention not only for their unmatched structural diversity,<sup>1,2</sup> but also for their potential applications in quite diverse disciplines including catalysis<sup>3,4</sup> and materials science,<sup>5</sup> as well as models for the examination of nucleation/growth processes.<sup>6</sup> Recent work has focused on the development of hybrid materials with POM-based clusters as structure directing units,<sup>7</sup> however, many of these examples are based on the traditional POM clusters *e.g.* Keggin or Wells-Dawson type and their lacunary fragments. Therefore, it is still a great challenge to discover new types of low nuclearity POM clusters that fall outside these classes. In our work we have been attempting to access new cluster types by manipulating variables such as pH, ionic strength, buffer capacity and cation type/size for example.<sup>8</sup> Recently, we have developed a new synthetic approach utilizing bulky organic amines, such as protonated hexamethylenetetraamine (HMTA) and triethanolammonium (TEA), as they can "shrink-wrap" the anionic clusters and allow us to isolate new polyoxometalate archetypes, such as  $[H_{12}W_{36}O_{120}]^{12-}$ ,  $[M_{18}O_{54}(SO_3)_2]^{4-}$  ( $M = Mo$  or  $W$ ),  $[H_4W_{19}O_{62}]^{6-}$ ,  $[H_3W_{18}O_{56}(IO_6)]^{6-}$  and a partially reduced cluster  $[H_2Mo^V_4Mo^VI_{12}O_{52}]^{10-}$ .<sup>8</sup> The extension of this work by selecting the multifunctional ligand *N,N'*-bis(2-hydroxyethyl) piperazine (BHPEP), which can serve as a buffer, encapsulating cation and a ligand, led to the discovery of an unprecedented dimeric cluster  $[(PMnW_{11}O_{39})_2(PO_4)]^{13-}$ .<sup>9</sup>

Here by using the protonated ligand  $H_2BHPEP^{2+}$ , we isolated a new POM architecture:  $(H_2BHPEP)_2Na_{10}\{[(P_4W_6O_{34})_2Co_2Na_2(H_2O)_2]\{Co(H_2O)_4\}_2\} \cdot 1.25H_2O$ ,§ which contains a heteropolyanion with unprecedented structural features, with the polyanions being connected covalently into chains by cobalt dimers, and then into three dimensions by sodium cations. The

phosphotungstate species observed in **1** can be formulated as  $[P_4W_6O_{34}]^{12-}$ , and is structurally related to the well known  $\{B-\alpha-PW_9O_{34}\}$  trilacunary heteropolyanion. In compound **1** (Fig. 1), the tungstate fragment is composed of three edge sharing  $\{W_2O_{10}\}$  units which are connected through corner sharing oxygen atoms to form a hexatungstate  $\{W_6O_{28}\}$  ring.<sup>10</sup> A phosphate group then decorates each of these  $\{W_2O_{10}\}$  units through a single  $\mu_2$ -oxo to each tungsten metal centre with six P–O bonds in the range 1.522(7)–1.572(6) Å, and six W–O bonds with lengths in the range 2.081(7)–2.196(8) Å.

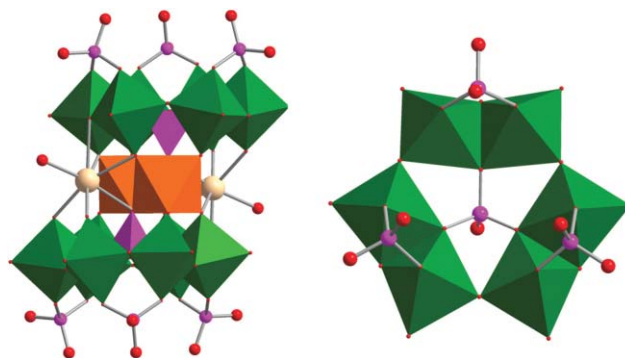


**Fig. 1** Left: structural representation of  $[P_4W_6O_{34}]^{12-}$ . Right: representation of the  $[P_4W_6O_{34}]^{12-}$  polyanion, clearly showing the corner sharing connectivity between the  $\{PW_2O_{12}\}$  triads.  $WO_6$  = green polyhedra,  $CoO_6$  = orange polyhedra,  $Na$  = cream spheres,  $PO_4$  = purple polyhedra,  $O$  = red spheres,  $P$  = purple spheres.

The two remaining oxygen ligands of the tetrahedral phosphate groups then point away from the cluster with one of the oxygen ligands involved in coordination to a  $\{Co_2(H_2O)_8\}$  unit which is discussed later. This type of coordination results in the formation of a  $\{W_2PO_{12}\}$  triad that is comparable with the  $\{W_3O_{13}\}$  triads that are a common feature of most polytungstate clusters, see Fig. 2.

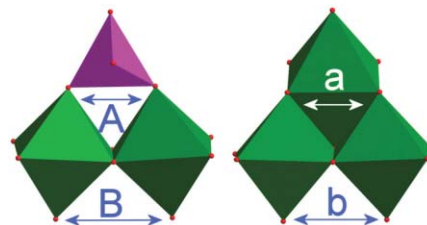


**Fig. 2** Representation of the  $\{W_2PO_{12}\}$  triad (left) found in compound **1** and a structural comparison with the common  $\{W_3O_{13}\}$  triad found in most polyoxotungstate clusters (right);  $A = 2.51$ ,  $B = 3.50$  compared to  $a = 2.65$  and  $b = 3.23$  Å;  $WO_6$  = green polyhedra,  $PO_4$  = purple polyhedra.

<sup>a</sup>WestCHEM, Department of Chemistry, University of Glasgow, Joseph Black Building, University Avenue, Glasgow, UK G12 8QQ. E-mail: L.Cronin@chem.gla.ac.uk; Fax: +44 141 330 4888; Tel: +44 141 330 6650

<sup>b</sup>Key Laboratory of Polyoxometalate Science of Ministry of Education, Department of Chemistry, Northeast Normal University, Changchun, Jilin, People's Republic of China. E-mail: linxu@nenu.edu.cn; Fax: +86 431 85099668; Tel: +86 431 85099668

† Electronic supplementary information (ESI) available: Additional experimental details. CCDC reference number 727740. For ESI and crystallographic data in CIF or other electronic format see DOI: 10.1039/b907410d

‡ Both authors contributed equally to this work.

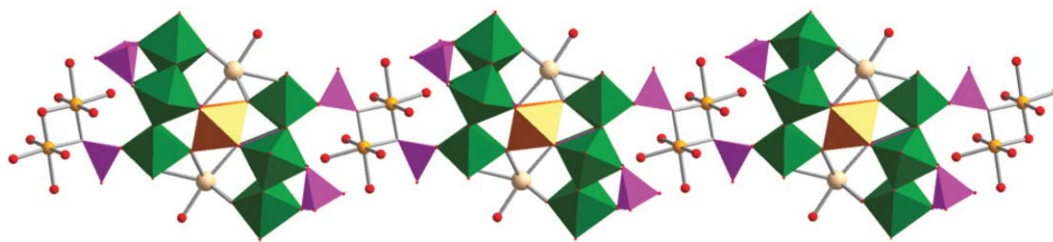


**Fig. 3** Connection of  $[P_8W_{12}Co_2Na_2O_{68}]^{18-}$  polyanions into 1D structures by cobalt dimers (top:  $WO_6$  = green polyhedra,  $CoO_6$  = orange polyhedra, Na = cream spheres,  $PO_4$  = purple polyhedra, O = red spheres).

When comparing each triad directly, the following structural differences are observed. Firstly, the two apical oxo ligands of the  $\{W_2\}$  units to which the phosphate is bound are pulled closer together than the corresponding positions in the  $\{W_3\}$  units, resulting in some strain within the triad and effectively causing the  $\{W_2O_{10}\}$  unit to be bent out of the plane to accommodate the phosphate. Three of these  $\{W_2PO_{12}\}$  triads then combine through an additional central phosphate to form the unique lacunary species, with the phosphate binding to each of the  $\{W_2PO_{12}\}$  fragments through a  $\mu_3$ -oxo with an average P-O bond length of 1.543 Å.

Two of these unique  $[P_4W_6O_{34}]^{12-}$  cluster units then coordinate to an additional  $\{Co_2Na_2\}$  fragment through the seven terminal W=O ligands on each of the lacunary species resulting in the formation of a sandwich complex. Each half of the sandwich complex is also crystallographically equivalent, due to the sandwiched cobalt ions being located on an inversion centre, with both of the cobalt centres being found to be in the +2 oxidation state according to bond valence sum calculations, structural and chemical analysis.

The extension of these clusters from molecules into 1D chains (Fig. 3) occurs through a dimeric cobalt species which binds to the clusters through two  $\mu_3$ -oxo ligands of the surface bound phosphate groups from two separate clusters, with a Co–Co distance of 2.803(6) Å and a Co–O–Co angle of 87.44(1)°, see Fig. 3.

As the cobalt atoms are separated by an inversion centre, their coordination environments are identical with both having octahedral coordination geometries, with aqua ligands filling the remaining coordination sites with the Co–OH<sub>2</sub> bond distances ranging 2.166(15)–2.212(17) Å for 6 of the 8 water ligands. The remaining two water ligands are ligated at the distance of 2.291(10) Å. In addition, the sodium cations are connected by BHEP through both hydroxyl groups of the ligand, forming wave-like chains. While polyanionic chains are further bridged through a Na–O–W linkage (Na–O: 2.231 Å, W–O: 1.730 Å) in the *ab* plane, showing a layer of the 3D hybrid framework (Fig. 4).

On heating the crystals, their colour is observed to change from pink to blue and then back to pink upon standing in an atmosphere of water vapour showing that the electronic environment of the cobalt centres are affected upon dehydration from  $1.8H_2O$  to  $1.0H_2O$  (from here on referred to as  $I_{hyd}$  and  $I_{dehyd}$ ). The colour change is also demonstrated by solid state UV/vis measurements, see ESI†). The solvated states of compounds **1** were determined by best fit of the elemental analysis (note the crystal structure shows substantially more water molecules present as solvent but the measurements on the samples was done on powdered, dry

material) and by careful inspection of the TGA, however it is not possible to distinguish between  $I_{hyd}$  and  $I_{dehyd}$  using elemental analysis alone. Also, the dehydrated compound  $I_{dehyd}$  does not retain crystallinity therefore preventing structural determination. Despite the lack of structural data we can postulate that the colour change could be associated with the weakly bound aqua ligand on the dimeric cobalt linkers which connects the polyanions into 1D chains. This type of process,<sup>11</sup> and blue Co<sup>II</sup>-substituted POM clusters,<sup>12</sup> are known.

However, according to the literature,<sup>12</sup> the colour change from pink to blue may be caused by the structural transformation/distortion of the Co centre from a six coordinate octahedral geometry to a five-coordinate, square based pyramidal, structure resulting from loss of one of the water ligands, or by solvation changes around the coordinated ligands. Thermogravimetric analysis of **1** exhibits a three-step weight loss that correlates with the loss of various components in the crystal structure. The initial weight loss of 9.07% over the temperature range of 30–110 °C accounts for solvent water molecules (calc. 9.04%). The second decomposition process is associated with the loss of all BHEP present in the structure between 200 and 400 °C. The final weight loss corresponds to the decomposition of the metal oxide to accommodate the complete oxidation of residual organic fragments that otherwise cannot be oxidised in the N<sub>2</sub> atmosphere. DSC analysis of **1** also agrees with the loss of water at 110 °C and the loss of BHEP at 380 °C.

Variable-temperature magnetic susceptibility of  $I_{hyd}$  and  $I_{dehyd}$  was collected with an applied field of 1000 Oe in the temperature range of 2–300 K. The  $\chi_m T$  vs. *T* plots are shown in Fig. 5 for the purposes of comparison (hence no detailed magnetic analysis is presented here), however inspection of the plots shows a drop in  $\chi_m T$  from 8.3 at room temperature to 7.76 and 7.08 emu mol<sup>-1</sup> K for  $I_{dehyd}$  and  $I_{hyd}$  respectively, see Fig. 5. Although a detailed magnetic analysis is not trivial due to the significant first-order orbital angular momentum contribution to the magnetic moment associated with high spin Co(II) species, inspection of the structure indicates the possibility of ferromagnetic interactions between the Co ions within the dimer, according to the small Co–O–Co angle of 87.46(1)°. Therefore it appears that the geometry change at the Co centres upon dehydration is supported also by the magnetic data, however this will need to be explored in detail in further studies. To quantify this further solid state UV/vis measurements were conducted that show that the original hydrated pink material has a broad absorption at *ca.* 560 nm which splits into two absorptions at *ca.* 538 and 584 nm in the dehydrated, blue, material. Exposure of the blue material to water vapour overnight regenerates the pink material and this is also demonstrated by UV/vis.

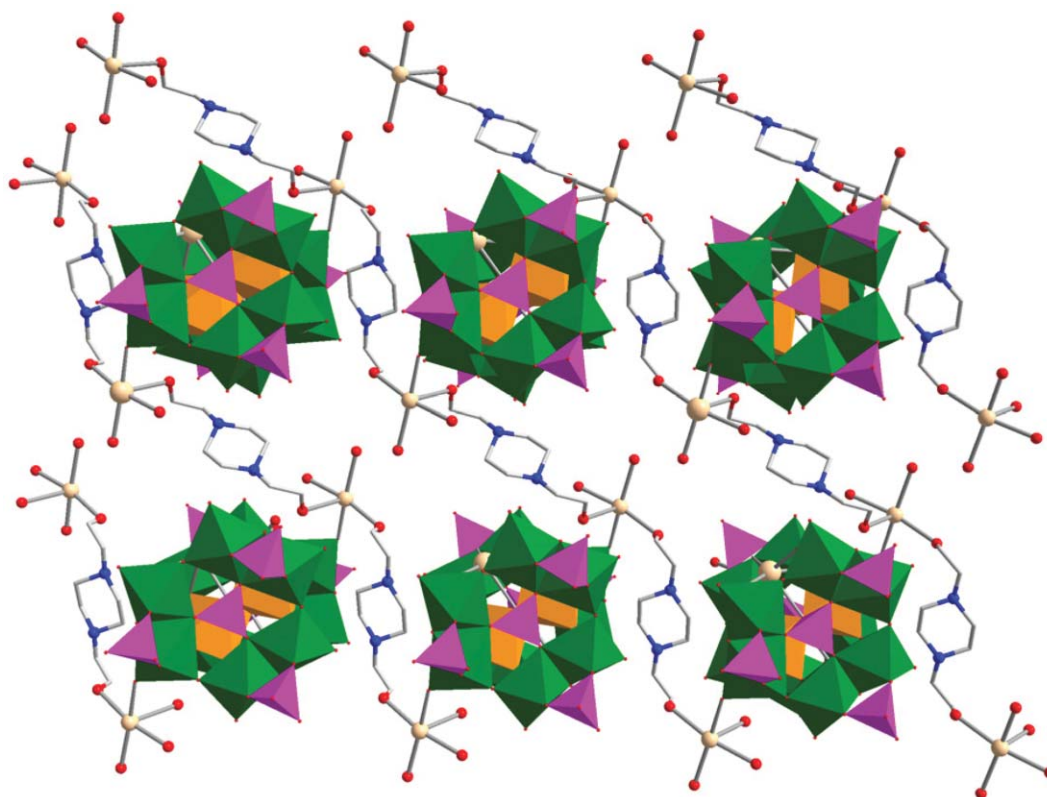


**Fig. 4** A 2D layer of the 3D network found in **1** showing the connectivity between  $[P_8W_{12}Co_2Na_2O_{68}]_n$  chains by  $Na^+$  and BHEP to form a 3D framework. Lattice water molecules were omitted for clarity.  $WO_6$  = green polyhedra,  $CoO_6$  = orange polyhedra,  $Na$  = cream spheres,  $PO_4$  = purple polyhedra,  $O$  = red spheres,  $P$  = purple spheres,  $C$  = grey sticks,  $N$  = blue spheres.

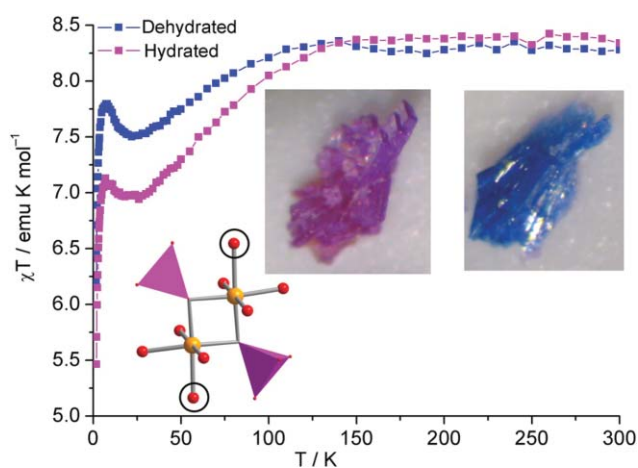


**Fig. 5** Temperature dependence of  $\chi_m T$  for **1** (hydrated) and **1'** (dehydrated). The cobalt dimer is shown with the two bridging phosphate groups and eight water molecules. The weakly bound water molecules are highlighted.  $Co$  = orange,  $O$  = red, phosphate = purple polyhedra.

In summary, by employing the multifunctional ligand *N,N'*-bis(2-hydroxyethyl)piperazine, a hybrid polyoxometalate framework based on a new heteropolyanion building block has been isolated successfully. This once again highlights the remarkable effect of cation nature in the isolation of new polyoxometalate archetypes. On dehydration, compound **1** undergoes a reversible colour change from pink to blue maybe owing to the geome-

try change, which affects the magnetic and UV/vis properties prominently. Future work will be concentrated on exploring the exact cause of the colour change and detailed magnetic and spectroscopic investigations.

## Notes and references

$\frac{1}{2} Na_2WO_4 \cdot 2H_2O$  (8.25 g, 25 mmol), was dissolved in 100 ml 1M NaCl and the pH was adjusted to 3.5 using 4M nitric acid. *N,N'*-Bis(2-hydroxyethyl)piperazine (4.75 g, 27 mmol) is then added followed by 85%  $H_3PO_4$  (2.05 g, 17.7 mmol). This solution is then stirred until all white precipitate redissolves, and  $Co(NO_3)_2 \cdot 6H_2O$  (2.18 g, 7.5 mmol) is added as solid. At this point a large amount of purple precipitate forms, and the solution is then heated to 75 °C and stirred vigorously until all this purple precipitate dissolves. A small amount of  $CoHPO_4$  is then separated by centrifugation after cooling to room temperature, with a final pH of 6.1. A small amount of  $(H_2bhep)_3Na_4[B-\alpha-P_2W_{18}Co_4O_{68}] \cdot 15H_2O$  is separated after 1 day. Finally, pale purple crystals of  $(H_2bhep)_{10}Na_{10}[P_8W_{12}Co_2Na_2(H_2O)_2O_{68}\{Co_2(H_2O)_4\}] \cdot 8H_2O$  form over a two weeks period. (Yield = 800 mg, 0.18 mmol, 8.68% based on W) Elemental analysis calcd (%),  $C_{16}H_{68}N_4Na_{12}Co_4O_{86}P_8W_{12}$ : C 4.13, H 1.47, N 1.20, Na 5.92; found: C 4.35, H 2.07, N 1.41, Na 5.92. Characteristic IR bands (KBr): 3445 (br), 1637 (m), 1467 (wk), 1384 (sh), 1124 (wk), 1056 (m), 1019 (w), 939 (m), 894 (m), 841 (m), 701 (m), 528 (w), 457 (w), 411 (w)  $cm^{-1}$ . Crystallographic data:  $(C_8H_{20}N_2O_2)_2Na_{10}\{(P_8W_{68}O_{34})_2Co_2Na_2(H_2O)_2\}\{Co_2(H_2O)_4\} \cdot 25H_2O$ ,  $M = 4964.52$  (note, only 4 Na positions found crystallographically), triclinic, space group *P*-1,  $a = 13.0887(11)$ ,  $b = 14.9813(14)$ ,  $c = 17.1216(16)$  Å,  $\alpha = 69.184(5)$ ,  $\beta = 70.767(5)$ ,  $\gamma = 86.494(5)^\circ$ ,  $V = 2957.1(15)$  Å<sup>3</sup>,  $Z = 1$ ,  $\mu(Mo-K\alpha) = 12.399$  mm<sup>-1</sup>. 42339 reflections measured, 10789 unique ( $R_{int} = 0.064$ ), 8164 observed reflections ( $I > 2\sigma(I)$ ), 662 refined parameters,  $R_1 = 0.0626$ ,  $wR_2 = 0.1901$ . Crystal data were measured on a Bruker ApexII CCD diffractometer using

Mo K $\alpha$  radiation ( $\lambda = 0.71073 \text{ \AA}$ ) at 100(2) K. CCDC 727740. Magnetic susceptibility data were recorded using a Quantum Design MPMS5-XL SQUID magnetometer.

- 1 D.-L. Long, E. Burkholder and L. Cronin, *Chem. Soc. Rev.*, 2007, **36**, 105.
- 2 L. Cronin, P. Kögerler and A. Müller, *J. Solid State Chem.*, 2000, **152**, 57.
- 3 N. Mizuno and K. Yamaguchi, *Coord. Chem. Rev.*, 2005, **249**, 1944.
- 4 C. L. Hill, *J. Mol. Catal. A: Chem.*, 2007, **262**, 2.
- 5 A. Müller and S. Roy, *Coord. Chem. Rev.*, 2003, **245**, 153.
- 6 A. Müller, S. Q. N. Shah, H. Bögge and M. Schmidtman, *Nature*, 1999, **397**, 48.
- 7 (a) A. Dolbecq, P. Mialane, L. Lisnard, J. Marrot and F. Sécheresse, *Eur. J. Inorg. Chem.*, 2003, 2914; (b) S. Reinoso, P. Vitoria, L. Lezama, A. Luque and J. M. Gutiérrez-Zorrilla, *Inorg. Chem.*, 2003, **42**, 3709; (c) Y. Ishii, Y. Takenaka and K. Konishi, *Angew. Chem., Int. Ed.*, 2004, **43**, 2702; (d) C. Streb, D.-L. Long and L. Cronin, *Chem. Commun.*, 2007, 471; (e) C. Streb, C. Ritchie, D.-L. Long, P. Kögerler and L. Cronin, *Angew. Chem., Int. Ed.*, 2007, **46**, 7579; (f) Y.-F. Song, D.-L. Long and L. Cronin, *Angew. Chem., Int. Ed.*, 2007, **46**, 390; (g) H. An, Y. Li, E. Wang, D. Xiao, C. Sun and L. Xu, *Inorg. Chem.*, 2005, **44**, 6062.
- 8 (a) D.-L. Long, P. Kögerler, L. J. Farrugia and L. Cronin, *Dalton Trans.*, 2005, 1372; (b) D.-L. Long, P. Kögerler, L. J. Farrugia and L. Cronin, *Angew. Chem., Int. Ed.*, 2003, **42**, 4180; (c) D.-L. Long, H. Abbas, P. Kögerler and L. Cronin, *J. Am. Chem. Soc.*, 2004, **126**, 13880; (d) D.-L. Long, P. Kögerler, A. D. C. Parenty, J. Fielden and L. Cronin, *Angew. Chem., Int. Ed.*, 2006, **45**, 4798; (e) D.-L. Long, O. Brücher, C. Streb and L. Cronin, *Dalton Trans.*, 2006, 2852; (f) D.-L. Long, Y. F. Song, E. F. Wilson, P. Kögerler, S. X. Guo, A. M. Bond, J. S. J. Hargreaves and L. Cronin, *Angew. Chem., Int. Ed.*, 2008, **47**, 4384; (g) D.-L. Long, P. Kögerler, L. J. Farrugia and L. Cronin, *Dalton Trans.*, 2005, 1372.
- 9 C. Ritchie, E. M. Burkholder, D.-L. Long, D. Adam, P. Kögerler and L. Cronin, *Chem. Commun.*, 2007, 468.
- 10 J. Wang, J. Zhao, P. Ma, J. Ma, L. Yang, Y. Bai, M. Li and J. Niu, *Chem. Commun.*, 2009, 2362.
- 11 L. Y. Wang, B. Zhao, C. X. Zhang, D. Z. Liao, Z. H. Jiang and S. P. Yan, *Inorg. Chem.*, 2003, **42**, 5804.
- 12 H. Liu, L. Xu, G. Gao, F. Li and N. Jiang, *J. Mol. Struct.*, 2008, **878**, 124.